

See discussions, stats, and author profiles for this publication at: <https://www.researchgate.net/publication/319980865>

# Effects of spread and local geometrical irregularities on the horizontal carrying capacity of masonry arches

Conference Paper · September 2017

CITATIONS

0

READ

1

6 authors, including:



[Nicola Cavalagli](#)

Università degli Studi di Perugia

39 PUBLICATIONS 91 CITATIONS

[SEE PROFILE](#)



[Paolo Zampieri](#)

University of Padova

23 PUBLICATIONS 68 CITATIONS

[SEE PROFILE](#)



[Nicolò Simoncello](#)

University of Padova

2 PUBLICATIONS 0 CITATIONS

[SEE PROFILE](#)



[Carlo Pellegrino](#)

University of Padova

179 PUBLICATIONS 1,671 CITATIONS

[SEE PROFILE](#)

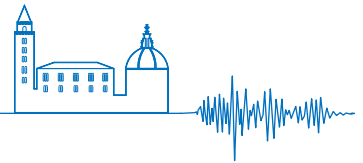
Some of the authors of this publication are also working on these related projects:



Fatigue strength of deteriorated steel joints [View project](#)



Seismic risk assessment of industrial productive processes - business interruption [View project](#)



# Effects of spread and local geometrical irregularities on the horizontal carrying capacity of masonry arches

Laura Severini<sup>a</sup>, Nicola Cavalagli<sup>a</sup>, Paolo Zampieri<sup>b</sup>, Nicolò Simoncello<sup>b</sup>, Vittorio Gusella<sup>a</sup>, Carlo Pellegrino<sup>b</sup>

<sup>a</sup> Dipartimento di Ingegneria Civile e Ambientale, Università degli Studi di Perugia, Perugia.

<sup>b</sup> Dipartimento di Ingegneria Civile, Edile e Ambientale, Università di Padova, Padova.

*Keywords: Masonry arch, Limit analysis, Geometrical irregularities, Damage, Seismic capacity.*

## ABSTRACT

The masonry arch is one of the main structural elements inside ancient buildings or bridges with relevant architectural or monumental value. Defects of shape of voussoirs due to inaccurate cutting of stones, imprecise construction or deterioration phenomena occurred during time, are often found inside historical constructions. In this context, an adequate safety assessment should consider the consequent reduction of carrying capacity, especially when dealing with buildings in seismic areas.

In this paper, two approaches for the modelling of geometrical irregularities on the masonry arch, both based on limit analysis, are presented and compared. In the first method, geometrical defect is spread over the whole arch, considering each voussoir geometry as uncertain in a probabilistic sense. A local damage is instead generated in the second approach through a thickness reduction at the intrados side. Effects of geometrical irregularities on the seismic capacity of the masonry arch are shown in terms of load multiplier and quantified through a safety factor.

## 1 INTRODUCTION

The architectural heritage is characterized by the presence of the masonry arch as a fundamental carrying element. The necessity of preservation and conservation of these ancient buildings requires a deep knowledge of the behaviour of the arch under applied loads, especially when dealing with seismic actions.

First studies on the stability of the masonry arch based on the limit analysis were carried out by Heyman during the XX century (Heyman 1969; Heyman 1982). In this context, the bearing capacity is usually considered a geometric problem and the shape of the arch and the voussoirs are assumed as deterministic (Cavalagli et al. 2016).

More recently, some authors analysed the effect of geometrical irregularities on the carrying capacity of the masonry arch, according to different approaches. De Arteaga and Morer (de Arteaga and Morer 2012), following Livesley's linear programming method combined

with a detailed structural relief of some cases study, analysed masonry arches subjected to a vertical pointed load, concluding that an idealized geometry may lead to an unsafe solution in term of collapse multiplier.

A limit analysis based procedure is referred Riveiro and co-authors. (Riveiro et al. 2013) and applied to an existing masonry arch bridge in order to study the influence of thickness value on collapse condition of the masonry arch. The influence of a local thickness reduction on the seismic capacity of masonry arches has been evaluated by Zampieri and co-authors (Zampieri et al. 2016a) by means of a limit analysis procedure based on the virtual work principle. Zanaz and co-authors (Zanaz et al. 2016), developed a methodology for the probabilistic assessment of the masonry vaults bearing capacity in presence of a pointed vertical load, based on the finite element method, considering a localized thickness loss of the arch. A different approach, based on limit analysis, has been proposed by Cavalagli and co-authors (Cavalagli et al. 2017), where geometrical uncertainties are

reproduced in a probabilistic sense considering geometrical parameters as random variables.

In this paper, two methods based on limit analysis and considering geometrical irregularities of the masonry arch are presented and compared. The first method reproduces a spread geometrical defect, considering geometrical parameters that define the shape of each voussoir as uncertain in a probabilistic sense. A local damage is instead modelled in the second approach by means of a thickness reduction at the intrados side of the arch. Effects of geometrical irregularities are investigated and quantified by a safety factor.

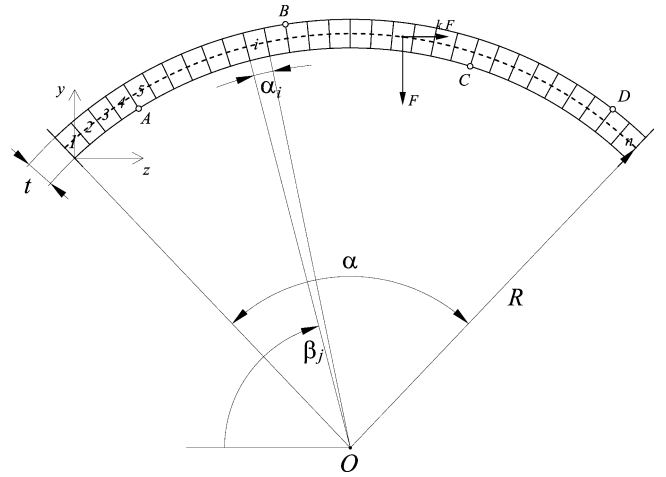


Figure 1. Geometrical parameters, loading system and generic configuration for collapse hinges.

## 2 A PROBABILISTIC APPROACH FOR MODELLING SPREAD GEOMETRICAL IRREGULARITIES

### 2.1 Limit analysis based method

The stability of the masonry arch is evaluated through limit analysis. A no-tension material, with infinite compressive strength, in the absence of sliding between the voussoirs, is considered (Heyman 1969). It is assumed that collapse occurs when the equilibrium, the mechanism and the yielding conditions are verified simultaneously. In other words, when the arch fails for the occurrence of a kinematic chain, a thrust line in equilibrium with the acting loads, lying inside the boundaries of the thickness and such as to determine a mechanism is found. The mechanism corresponds to the formation of hinges at the intrados and extrados side of the arch, the number of which depends on the geometry and on the loading system (Cavalagli et al. 2016, Zampieri et al. 2016b).

### 2.2 Geometrical description

The nominal (or deterministic) geometry of the masonry arch is circular and defined by assigning the radius  $R$ , the angle of embrace  $\alpha$  and the thickness  $t$ . The arch is discretized into  $n$  voussoirs by radial lines passing through the origin  $O$  (Figure 1), corresponding to a stereometry parameter  $\eta = \alpha/n$ . The geometry of the generic  $i$ th voussoir is identified by means of the angle of embrace  $\alpha_i$ , the thickness  $t_i$  and the radius  $R_i$  of the mean circular construction line of the voussoir itself.

Geometrical irregularities are modelled under the following assumptions (Cavalagli et al. 2017): *i*) radial joints, *ii*) deterministic value of the angle of embrace  $\alpha$  of the arch and *iii*) the angle of embrace  $\alpha_i$ , the thickness  $t_i$  and the radius  $R_i$  of each voussoir are random variables with uniform probability density functions (independent functions):

$$\begin{aligned}\alpha_i &= E[\alpha_i] + \varepsilon \alpha / n \cdot p_{\alpha_i} = \alpha / n + \varepsilon \alpha / n \cdot p_{\alpha_i} \\ \tilde{t}_i &= E[\tilde{t}_i] + \varepsilon t \cdot p_{t_i} = t + \varepsilon t \cdot p_{t_i} \\ R_i &= E[R_i] + \chi R \cdot p_{R_i} = R + \chi R \cdot p_{R_i}\end{aligned}\quad (1)$$

where  $\varepsilon$  is the tolerance,  $\chi = \varepsilon t / R$  and  $p_{\alpha_i}$ ,  $p_{t_i}$ ,  $p_{R_i}$  are independent samples taken from a uniform probability density function defined in the range  $[-1,1]$ . The mean values of the random variables are assumed equal to the nominal ones.

In this paper, the results related to a nominal arch with angle of embrace  $\alpha = 157.5^\circ$  and dimensionless thickness  $t/R = 0.15$  are shown. Geometrical irregularities of the voussoirs are generated assuming values of the tolerance  $\varepsilon$  equal to 0.03, 0.05, 0.10. The discretization is carried out assuming several values of the number  $n$  of voussoirs, by varying it in the range 3-210 ( $1/\eta = 1.1-76.4$ ); at each value of  $n$ , a sample of  $h = 1000$  random arches is generated according to the Equations (1).

### 2.3 Loading system

The stability of the masonry arch is studied considering the action, on the generic voussoir, of

the self-weight  $F$  and the horizontal load  $F_s = k F$  proportional to the weight by means of the load multiplier  $k$  (Figure 1). The horizontal load is assumed directed from left to right in the calculations. The asymmetric loading condition implies that four-hinges are sufficient to activate the mechanism.

#### 2.4 Limit analysis procedure

The horizontal load multiplier  $k$  and the corresponding collapse mechanism are evaluated through an iterative procedure based on the limit analysis (Cavalagli et al. 2016). A first attempt position for the collapse hinges  $A, B, C, D$  is assigned (Figure 1), i.e. a collapse mechanism is assumed. Then, the equilibrium of moments around three hinges is imposed:

$$\begin{cases} H_D(y_A - y_D) + V_D(z_A - z_D) - \sum_{i=1}^{n_{AD}} F_i(z_A - z_{G_i}) - k \cdot \sum_{i=1}^{n_{AD}} F_i(y_A - y_{G_i}) = 0 \\ H_D(y_B - y_D) + V_D(z_B - z_D) - \sum_{i=1}^{n_{BD}} F_i(z_B - z_{G_i}) - k \cdot \sum_{i=1}^{n_{BD}} F_i(y_B - y_{G_i}) = 0 \\ H_D(y_C - y_D) + V_D(z_C - z_D) - \sum_{i=1}^{n_{CD}} F_i(z_C - z_{G_i}) - k \cdot \sum_{i=1}^{n_{CD}} F_i(y_C - y_{G_i}) = 0 \end{cases} \quad (2)$$

where  $n_{AD}$ ,  $n_{BD}$ ,  $n_{CD}$  refer respectively to the number of voussoirs between the hinges  $A, B, C$  and  $D$ . System of Equations (2) can be solved in order to determine the horizontal loads multiplier  $k$ . Finally, the thrust line is determined through the calculation of the eccentricity  $e_j$  of the normal force at each joint; then, the yielding criterion is checked:

$$-\frac{t_j}{2} \leq e_j \leq +\frac{t_j}{2} \quad (3)$$

If the thrust line is not contained everywhere inside the boundaries of the arch geometry, Equation (3) is not verified. In this case a new trial configuration of hinges has to be considered and the equilibrium imposed again.

It should be noted that when geometrical irregularities are modelled, the horizontal load multiplier becomes a random variable. For the generic random arch two values of the horizontal load multiplier can be determined, denoted as  $k_l$  and  $k_r$ , because the geometry is not symmetric respect to the vertical axis passing through the crown. Hence, the limit analysis has to be carried out considering both directions for the horizontal loads and the horizontal load multiplier is determined as follows

$$k = \min(k_l, k_r) \quad (4)$$

#### 2.5 Horizontal load multiplier for the arch with spread geometrical irregularities

The horizontal load multiplier and the corresponding collapse mechanism are evaluated for the nominal arch and for the generated samples of random arches, while varying the number of voussoir  $n$ , by means of the limit analysis procedure previously described at paragraph §2.4.

Let us denote as  $k_{nom}$  the load multiplier for the nominal arch when  $n \rightarrow \infty$ , i.e. the solution related to a continuous medium. For an assigned value of  $\eta$ , at each case  $h$ , with  $h=1-1000$ , three independent sets of samples  $\alpha_i$ ,  $\tilde{t}_i$ ,  $R_i$  are generated, according to the Equations (1). Then, the corresponding value of the random horizontal load multiplier  $k$  is evaluated. In Figure 2 the histogram of the probability density of the horizontal load multiplier  $k$  is represented for  $\varepsilon = 0.10$ , with its interpolant normal probability density function (continuous black line), superimposed to the interpolant normal probability density functions of  $k_l$  (dashed black line) and  $k_r$  (dash-dot black line). The nominal multiplier  $k_{nom}$  is indicated by means of a blue vertical line. It can be observed that the mean and the standard deviations values of the random variables  $k_l$  and  $k_r$  are very closed. Moreover, the mean value of the interpolant normal probability density function, depicted by the vertical continuous black line, is lower than the nominal value, revealing the main effect of the modelled geometrical spread irregularities. The analysis is repeated for several values of the number of voussoirs. At each one of them, the mean value and the standard deviation of the random load multiplier are determined. A safety factor is introduced to quantify the effects of spread geometrical irregularities at each value of the stereometry parameter:

$$\gamma_s(\eta) = \frac{E[k_\eta] - \sigma[k_\eta]}{k_{nom}} \quad (5)$$

where  $E[k_\eta]$  is the mean value of the random load multipliers of the generated 1000 random arches and  $\sigma[k_\eta]$  is the standard deviation for a discretization with  $n = \alpha / \eta$  voussoirs. The results

in terms of safety factor are presented in Figure 3 depending on the stereometry parameter. A reduction of the horizontal load multiplier is obtained when geometrical irregularities are considered.

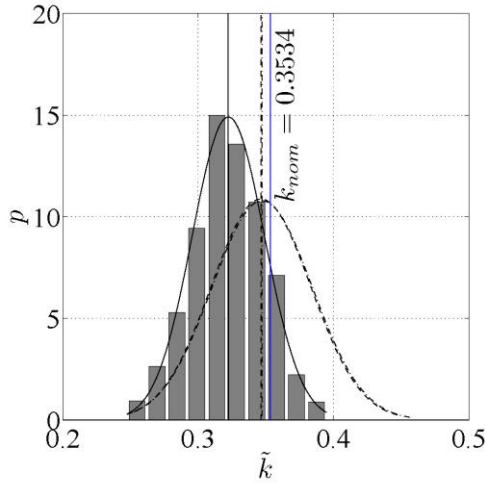


Figure 2. Histogram of the probability density of the horizontal loads multiplier  $k$  with its interpolant normal probability density function (continuous black line) and with the indication of the nominal horizontal loads multiplier (blue line), superimposed to the interpolant normal probability density functions of  $k_l$  (dashed black line) and  $k_r$  (dash-dot black line), for  $\varepsilon = 0.10$ . Case number of voussoir  $n = 5$  (Cavalagli et al. 2017).

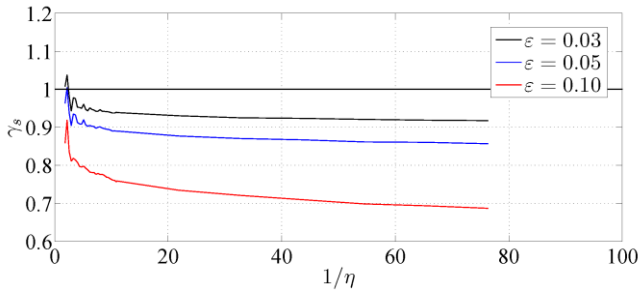


Figure 3. Safety factor depending on the stereometry parameter at several value of the tolerance  $\varepsilon$  (Cavalagli et al. 2017).

### 3 MODELLING OF LOCAL GEOMETRICAL IRREGULARITIES

#### 3.1 Geometrical description

Arch local thickness reduction is a typical defect of masonry bridges and it is the consequence of different actions applied to the structure (Harvey 2012). For example, it can be generated by: the collision between arch and

vehicle, loss of brick, the action of cycled load etc.

Local geometrical irregularity can be represented in the limit analysis model by defining three parameters (Figure 4) that establish its intensity, its position and its localization (Kaminski and Bien 2013; Zampieri et al. 2016a). If  $t$  and  $S$  are the thickness and length of the arch, the intensity of the reduction in arch thickness can be defined using the following relationship:

$$Intensity = \frac{\Delta t}{t} \quad (6)$$

The extent of the defect can be defined using the following relationship:

$$Extension = \frac{\Delta S}{S} \quad (7)$$

and the localization of the defect is given by the following angular relationship:

$$Localization = \frac{\beta_\sigma}{\alpha} \quad (8)$$

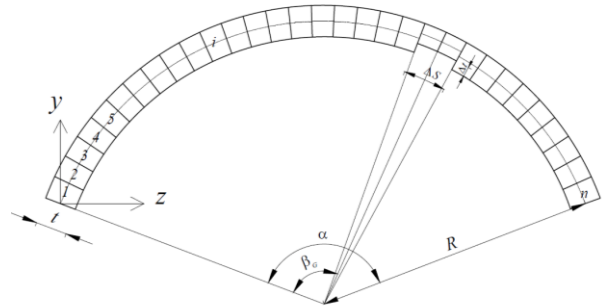


Figure 4. Representation of the arch that define the intensity, localization and extent of the defect on the arch.

In according with the parameters already explained before, an iterative algorithm, in order to calculate the collapse multiplier for horizontal loads of arch with local thickness reduction has been developed. Considering the arch geometry defined at paragraph §2.2, the load multiplier of damaged arch ( $k_{LR}$ ) it has been compared with that of intact arch ( $k$ ) considering different intensity, extension and position of arch local thickness reduction. In order to take into account the geometry of defect, a safety factor  $\gamma_s$  to be applied to  $k$  is proposed:

$$\gamma_s = \frac{k_{LR}}{k} \quad (9)$$

### 3.2 Parametrical analysis of masonry arch with local geometrical defect

A parametrical analysis is proposed with the aim to understand the influence of local geometry defect on lateral load carrying capacity of masonry arch. In this case, the parameters (Table 1) that vary are: the localization  $\beta_G/\alpha$ , the intensity  $\Delta t/t$ , and the extension  $\Delta S/S$  of the defect. The results of sensitive analysis are summarized in Figures 5, 6 and 7.

Table 1 Values of intensity, extension and localization of thickness local reduction used in parametrical analysis

Par.	values [-]							
$\Delta S/S$	0.01	0.02	0.03					
$\Delta t/t$	0.10	0.20	0.30					
$\beta_G/\alpha$	0.55	0.60	0.65	0.70	0.75	0.80	0.85	0.90

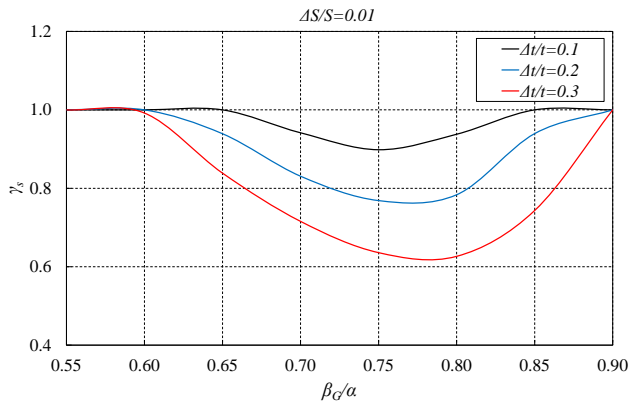


Figure 5. Safety factor function of  $\beta_G/\alpha$  for three levels of intensity ( $\Delta t/t=0.1, 0.2, 0.3$ ) and extension equal  $\Delta S/S=0.01$ .

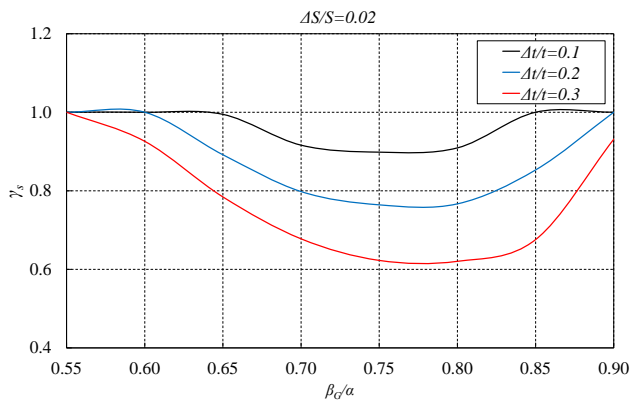


Figure 6. Safety factor function of  $\beta_G/\alpha$  for three levels of intensity ( $\Delta t/t=0.1, 0.2, 0.3$ ) and extension equal  $\Delta S/S=0.02$

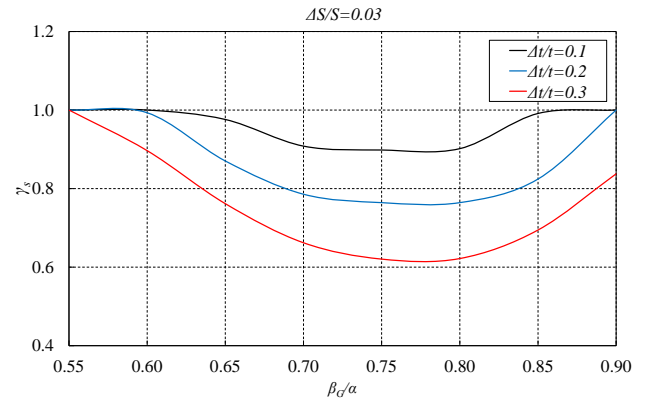


Figure 7. Safety factor function of  $\beta_G/\alpha$  for three levels of intensity ( $\Delta t/t=0.1, 0.2, 0.3$ ) and extension equal  $\Delta S/S=0.03$

Graphs in Figures 5, 6 and 7, for each considered level of  $\Delta S/S$ , describe the value of the safety factor depending to  $\beta_G/\alpha$  for three levels of defect intensity ( $\Delta t/t=0.1, 0.2, 0.3$ ). Observing the graphs it can be noted, from the comparison between the different curves referring to the three levels of  $\Delta t/t$ , that the influence of  $\Delta t/t$  on the value of  $\gamma_s$  is significant. From the graphs it can be also noted how once having specified a certain value of  $\Delta t/t$ , the reduction in the collapse multiplier depends both on the position of the defect  $\beta_G/\alpha$ . In fact, the presence of the defect can modify the position of hinges A B C and D compared the position of the hinges in seismic limit analysis of an intact arch. The defect's extension  $\Delta S/S$  influences the value of  $\gamma_s$  less than other parameters ( $\Delta t/t$  and  $\beta_G/\alpha$ ) indeed the minimum value of  $\gamma_s$  for the three different curves in Figure 5, 6 and 7 depends only by  $\Delta t/t$  and  $\beta_G/\alpha$ .

At the end is important underline that the presence of local thickness reduction in masonry decies the lateral load carrying capacity of the arch; in fact, if  $\beta_G/\alpha$  is equal to 0.75 the safety factor is equal to: 0.89 for  $\Delta t/t=0.1$ , 0.77 for  $\Delta t/t=0.2$  and 0.62 for  $\Delta t/t=0.3$ . In the last case the error, that it can be committed if the defect it not considered in the analysis, is about 40%.

## 4 REMARKS AND DISCUSSIONS

The proposed methods deal with the effects of geometrical irregularities on the stability of the masonry arch according to different approaches. In particular, different types of action are assumed to generate different types of defect. The first method, described at paragraph §2,

reproduces a spread uncertainty, related to defects of shape of the voussoirs due to imprecise construction or environmental actions. On the other hand, the second method, presented at paragraph §3, evaluates the effects of a local damage that could be associated to an impact or a loss of bricks. In reality, both phenomena could occur independently, causing a further reduction of stability for the arch. In other words, values of the safety factor less than those calculated separately for spread and local defects can be expected.

## 5 CONCLUSIONS

In this paper, the effects of geometrical irregularities on the stability of the masonry arch have been evaluated in presence of horizontal loads, according to different approaches. Two methods based on the limit analysis have been proposed and compared.

With the first method, spread geometrical irregularities have been generated according to a probabilistic approach, assuming the angle of embrace, the thickness and the mean radius of each voussoir as random variables. On the other hand, the second method reproduces a deterministic local damage, defined by thickness reduction and damage extension.

A safety factor has been proposed to quantify the loss of bearing capacity. Results have shown the reduction of stability of the masonry arch due to both types of geometrical defect, spread and local. In order to obtain an adequate safety assessment, actual geometry of the masonry arch should be modelled considering the superposition of spread and local geometrical irregularities. Therefore, in this condition a further reduction of bearing capacity can be expected.

## REFERENCES

- Cavalagli, N., Gusella, V., Severini, L., 2016. Lateral loads carrying capacity and minimum thickness of circular and pointed masonry arches, *International Journal of Mechanical Sciences*, **115-116**, 645-656.
- Cavalagli, N., Gusella, V., Severini, L., 2017. The safety of masonry arches with uncertain geometry, *Computer and structures*, **188**, 17-31.
- de Arteaga, I., Morer, P., 2012. The effect of geometry on the structural capacity of masonry arch bridges, *Construction and Building Materials*, **34**, 97-106.
- Heyman, J., 1969. The safety of masonry arches, *International Journal of Mechanical Sciences*, **11**, 363-385.
- Heyman, J., 1982. *The masonry arch*, Ellis Horwood Ltd, Chichester.
- Harvey, W.J., 2012. Stiffness and damage in masonry bridges. *The Structural Engineer*, **165(3)**, 127–134.
- Kaminski, T., Bien, J., 2013. Application of Kinematic Method and FEM in Analysis of Ultimate Load Bearing Capacity of Damaged Masonry Arch Bridges, 11th International Conference on Modern Building Materials, Structures and Techniques, MBMST 2013.
- Riveiro, B., Solla, M., Arteaga, I. de, Arias, P., Morer, P., 2013. A novel approach to evaluate masonry arch stability on the basis of limit analysis theory and non-destructive geometric characterization, *Automation in Construction*, **31**, 140-148.
- Zampieri, P. Zanini, M. A., Faleschini F., 2016a. Influence of damage on the seismic failure analysis of masonry arches. *Construction and Building Materials*, **119**, 343-355.
- Zampieri, P. Zanini, M. A., Faleschini F., 2016b. Derivation of analytical seismic fragility functions for Common Masonry Bridge types: Methodology and application to real cases. *Engineering failure analysis*, **68**, 275–291.
- Zanaz, A., Yotte, S., Fouchal, F., Chateauneuf, A., 2016. Efficient masonry vault inspection by Monte Carlo simulations: Case of hidden defect, *Case Studies in Structural Engineering*, **5**, 1-12.